Available online at www.sciencedirect.com
ScienceDirect
Biochimica et Biophysica Acta 1778 (2008) 250–259
Biochimica et Biophysica Acta
BBA
www.elsevier.com/locate/bbamem

uPA binding increases UPAR localization to lipid rafts and modifies the receptor microdomain composition

Macarena Sahores [a,b,c,1], Alessandro Prinetti [d], Gustavo Chiabrando [c], Francesco Blasi [a,b,*], Sandro Sonnino [d,*]

[a] *Molecular Genetics Unit, DIBIT, H. S. Raffaele, Department of Molecular Biology and Functional Genomics, Università Vita Salute San Raffaele, via Olgettina 60, 20132 Milan, Italy*
[b] *IFOM (FIRC Institute of Molecular Oncology), via Adamello 16, 20139 Milan, Italy*
[c] *Department of Clinical Biochemistry, CIBICI-CONICET, Faculty of Chemical Sciences, National University of Córdoba, Haya de la Torre y Medina Allende, Ciudad Universitaria, 5000, Córdoba, Argentina*
[d] *Center of Excellence on Neurodegenerative Diseases, Department of Medical Chemistry, Biochemistry and Biotechnology, University of Milan, 20090 Segrate, Italy*

Received 22 April 2007; received in revised form 6 September 2007; accepted 27 September 2007
Available online 6 October 2007

Abstract

UPAR is a GPI anchored protein, which is found in both lipid rafts and in more fluid regions of the plasma membrane. We have studied the role of the ligand uPA on uPAR localization and on the composition of the lipid membrane microdomains. We have analyzed the glycosphingolipid environment of uPAR in detergent resistant membrane (DRM) fractions prepared by cell lysis with 1% Triton X-100 and fractionated by sucrose gradient centrifugation obtained from HEK293-uPAR cells. The uPAR specific lipid membrane microdomain has been separated from the total DRM fraction by immunoprecipitation with an anti-uPAR specific antibody under conditions that preserve membrane integrity. We have also tested uPA-induced ERK phosphorylation in the presence of methyl-β-cyclodextrin, which is known to disrupt lipid rafts by sequestering cholesterol from such domains. Our results show that uPAR is partially associated with DRM and this association is increased by ligands, is independent of the catalytic activity of uPA, and is required for intracellular signalling. In the absence of ligands, uPAR experiences a lipid environment very similar to that of total DRM, enriched in sphingomyelin and glycosphingolipids. However, after treatment of cells with uPA or ATF the lipid environment is strongly impoverished of neutral glycosphingolipids.

Keywords: Urokinase receptor; Lipid raft; Immunoprecipitation; Urokinase

Abbreviations: Ganglioside and glycosphingolipid nomenclature is in accordance with Svennerholm, 1980 [1], and the IUPAC-IUBMB recommendations [2,3]. GlcCer, β-Glc-(1-1)-Cer; LacCer, β-Gal-(1-4)-β-Glc-(1-1)-Cer; GM3, II^{3}Neu5AcLacCer, α-Neu5Ac-(2-3)-β-Gal-(1-4)-β-Glc-(1-1)-Cer; GM2, II^{3}Neu5AcGgOse$_3$-Cer, β-GalNAc-(1-4)-[α-Neu5Ac-(2-3)]-β-Gal-(1-4)-β-Glc-(1-1)-Cer; GM1, II^{3}Neu5AcGgOse$_4$Cer, β-Gal-(1-3)-β-GalNAc-(1-4)-[α-Neu5Ac-(2-3)]-β-Gal-(1-4)-β-Glc-(1-1)-Cer; Cer, Ceramide, *N*-acyl-sphingosine; Sph, Sphingosine, (2*S*,3*R*,4*E*)-2-amino-1,3-dihydroxy-octadecene; [1-^{3}H]sphingosine, (2*S*,3*R*,4*E*)-2-amino-1,3-dihydroxy-[1-^{3}H]octadecene; PE, Phosphatidylethanolamine; SM, Sphingomyelin; SL, Sphingolipids; 2D-HPTLC, Two-dimensional high-performance thin layer chromatography; uPA, Urokinase plasminogen activator; uPAR, Urokinase receptor; ATF, Amino terminal fragment of uPA; TfR, Transferrin receptor; DRM, Detergent-resistant membranes; DS, Detergent-soluble material; GPI, Glycosylphosphatidylinositol; TX-100, Triton X-100; CHO, Cholesterol; CD, Methyl-β-cyclodextrin

* Corresponding authors. F. Blasi is to be contacted at Università Vita Salute San Raffaele, via Olgettina 60, 20132 Milan, Italy. Tel.: +39 02 26434744; fax: +39 0226434844. S. Sonnino, Department of Medical Chemistry, Biochemistry and Biotechnology, University of Milan, Via Fratelli Cervi, 20090 Segrate, Italy. Tel.: +39 02 50330360; fax: +39 0250330365.
E-mail addresses: blasi.francesco@hsr.it (F. Blasi), sandro.sonnino@unimi.it (S. Sonnino).
[1] Present address: Department of Anatomy and Developmental Biology, University College London, University Street, Rockefeller Building, London, WC1E 6BT, UK.

0005-2736/$ - see front matter © 2007 Published by Elsevier B.V.
doi:10.1016/j.bbamem.2007.09.030

1. Introduction

Extracellular proteolysis is a key element in diverse cellular processes including cell adhesion, proliferation and migration. These processes are involved in tissue remodelling, inflammation and tumour progression. The urokinase receptor (uPAR/CD87), by binding its specific ligand uPA at the cell surface allows the conversion of plasminogen into plasmin with the consequent degradation of the extracellular matrix. UPAR is a heterogeneously glycosylated protein of 45–55 kDa, inserted into the external leaflet of the plasma membrane through a glycosylphosphatidylinositol (GPI) anchor [4]. UPAR is able to activate different signal transduction pathways inside the cell, events that are dependent on uPA binding, but in some cases independent of the catalytic activity of uPA [5]. Since uPAR lacks a transmembrane domain, the signalling events triggered after uPA binding might be explained considering that uPAR can interact with other proteins either directly or as part of a multiprotein complex. Among the proteins that associate with uPAR, integrins, FPRL1 (a homologue of the fMLP receptor, FPR), LRP-1 (low-density lipoprotein–receptor-related protein), EGF-R (Epidermal Growth Factor Receptor), caveolin-1, and vitronectin can be mentioned. Through these associations uPAR can modify the state of the cell, controlling cell adhesion, migration and proliferation [5].

As other GPI-anchored proteins, uPAR is enriched in lipid rafts [6,7]. Lipid rafts or lipid membrane microdomains have been biochemically characterized by their resistance to solubilization with non ionic detergents at low temperatures [8,9]. These conditions lead to the isolation of detergent-resistant membranes (DRM), which have been extensively used in order to study lipid raft composition and function. DRMs are highly enriched in cholesterol and sphingolipids, such as sphingomyelin, ceramide and glycosphingolipids [8,10,11]. Because of their composition, lipid rafts are more ordered and less fluid than other regions of the plasma membrane [8,12]. These lipid membrane microdomains are also typically enriched, temporarily or permanently, in some proteins. These include integral membrane proteins, such as caveolins, flotillins and VIP36, GPI-anchored proteins like PLAP and Thy-1, some transmembrane proteins such as growth factor receptor tyrosine kinases, and signalling effectors such as G proteins and Src-family tyrosine kinases [13,14]. Lipid rafts have been involved in signal transduction events, vesicular trafficking, protein sorting and entrance of intracellular pathogens [13–16].

No information is available concerning the biochemical nature of uPAR environment within lipid rafts. The aim of this study was to identify and characterize the lipid rafts in which uPAR is located at steady-state conditions, i.e. in the absence of its extracellular ligand uPA. We also wanted to investigate whether the cell membrane microenvironment in which uPAR is located is modified after receptor activation by its ligand uPA (or ATF, the amino terminal, proteolytically inactive fragment of uPA). In this paper we analyze some aspects of the lipid composition of membrane fractions immunoprecipitated with a specific anti uPAR antibody, from a detergent-resistant, cholesterol- and sphingolipid-enriched membrane fraction prepared from epithelial cells. We demonstrate that uPAR is partially associated to the detergent-resistant membranes (DRM) obtained from HEK293-uPAR cells, and that after uPA binding there is a 3-fold increase in uPAR association to the DRM. We also show that uPA or ATF binding enrich the cell membrane microenvironment in which uPAR is located of sphingomyelin and gangliosides, while depleting it of neutral glycosphingolipids. The functional relevance of the presence of uPAR in lipid microdomains is shown by the complete inhibition of uPA intracellular signalling in methyl-β-cyclodextrin (CD)-treated cells in which lipid rafts are disrupted. We conclude that uPAR is located in specific subdomains within lipid rafts, the composition of which as well as uPAR distribution in the plasma cell membrane is regulated by its ligand uPA.

2. Materials and methods

2.1. Materials

Cell culture media and supplements were purchase from Gibco-BRL (Carlsbad, CA, USA) and plastic ware was from Costar (Cambridge, MA, USA). Triton X-100, methyl-β-cyclodextrin and general laboratory chemicals were from Sigma-Aldrich (St. Louis, MO, USA). Secondary HRP-conjugated antibodies and Redivue L-[^{35}S]methionine were from Amersham Pharmacia Biotech (Buckinghamshire, UK). PVDF membranes were from Millipore (MA, USA). Chemoluminescent substrate was from Pierce (IL, USA). Clinical grade uPA was obtained from Crinos (Italy). The R4 anti-uPAR antibodies were kindly provided by Dr. Gunilla Høyer-Hansen (Finsen Laboratory, Copenhagen, Denmark). The polyclonal anti-uPAR antibodies as well as ATF (the Amino Terminal Fragment of uPA) were produced and tested in our laboratory [6]. The monoclonal antibodies to Transferrin Receptor were purchased from Zymed Laboratories (S. San Francisco, CA, USA). The rabbit polyclonal antibodies to Caveolin-1 were obtained from Santa Cruz Biotechnology, Inc. (Santa Cruz, CA, USA). The rabbit polyclonal antibodies to Phospho-p44/42 MAP Kinase were purchased from Cell Signalling Technology, Inc. (Danvers, MA, USA), while the rabbit polyclonal antibodies to total ERK were from Santa Cruz Biotechnology, Inc. Protein G-Sepharose beads were from Amersham Pharmacia Biotech (Buckinghamshire, UK). Protein G-coupled magnetic beads (Dynabeads) were from Dynal ASA (Smestad, Oslo, Norway). Sphingosine was prepared from cerebroside [40]. [1-^{3}H]sphingosine was prepared by specific chemical oxidation of the primary hydroxyl group of sphingosine followed by reduction with sodium boro[^{3}H]hydride [41] (radiochemical purity over 98%; specific radioactivity 2 Ci/mmol). Tritiated lipids were extracted from [1-^{3}H]sphingosine-fed cells, purified, characterized and used as chromatographic standards. Sphingolipids and glycerolipids to be used as standards were extracted from rat brain, purified and characterized [42].

2.2. Cell culture

HEK293 cells stably transfected with human uPAR were cultured in Dulbecco's Modified Eagle Medium supplemented with penicillin (100 U/ml), streptomycin (100 U/ml), glutamine (5 mM), G418 (0.8 mg/ml) and 10% fetal bovine serum at 37 °C in 5% CO_2.

2.3. Metabolic radiolabeling

HEK 293-uPAR cells were incubated with 3.7×10^{-8} M [1-^{3}H]sphingosine (16 ml/162 cm^2 flask) in culture medium for 2 h. After the pulse, medium was replaced with fresh culture medium without radioactive sphingosine and cells were chased for 48 h. Under these conditions, all sphingolipids (including ceramide, sphingomyelin, neutral glycolipids and gangliosides) and phosphatidylethanolamine (obtained by recycling of radioactive ethanolamine formed in the catabolism of [1-^{3}H] sphingosine) are metabolically radiolabelled [43].

In order to radiolabel proteins, cells were incubated in methionine-free medium for 2 h and subsequently incubated in the presence of 17 μCi/ml L-[^{35}S] methionine for 20 h.

2.4. Purification of detergent-resistant membranes (DRM)

HEK 293-uPAR cells were plated at 70% confluence and lipids and proteins were metabolically radiolabelled with [1-^{3}H]sphingosine or L-[^{35}S]methionine, respectively, as described above. After metabolic radiolabeling, cells were washed twice with cold PBS, collected by scraping and centrifuged 5 min at 1200 rpm. Cells were lysed for 30 min on ice in ice-cold buffer A (150 mM NaCl, 2 mM EDTA, 50 mM Tris–HCl, pH 7.5) containing 1% TX-100 and a cocktail of proteinase inhibitors (Complete, Roche, Basel, Switzerland). Cell lysates were centrifuged at 4 °C for 5 min at 1200×*g*. One ml of this postnuclear supernatant was brought to 40% sucrose using 80% sucrose in buffer A plus detergent, placed at the bottom of a ultracentrifuge tube (Beckman Instruments Inc, Fullerton, CA, USA) and overlaid with 4 ml of 30% sucrose and 2 ml of 5% sucrose in buffer A plus detergent, and filled up with 4 ml of buffer alone. Samples were centrifuged at 4°C for 17 h at 39,000 rpm (Beckman ultracentrifuge rotor SW41Ti). After centrifugation, 1 ml fractions were collected from the top to the bottom of the gradient using a pipette. Eight fractions were collected. Fractions 2 and 3 were determined to correspond to DRM and fractions 7 and 8 to detergent soluble material (DS).

The sucrose density fractions obtained were analyzed to determine the protein distribution (by running the same fraction volume in SDS-PAGE followed by immunoblotting) as well as the content and distribution of radiolabelled lipids as described below.

2.5. Analysis of protein patterns

Cell lysates and sucrose gradient fractions obtained after labelling cells with [^{35}S]methionine were analyzed to determine protein content and pattern. Similar volumes of each sucrose density fraction were subjected to SDS-PAGE on 10% acrylamide gels followed by immunoblotting.

2.6. ERK phosphorylation

To perform time course analysis, HEK 293-uPAR cells (80% confluence) were serum-starved for 16 h and then incubated with 10 nM uPA for the indicated times at 37 °C. Then cells were washed with cold PBS and lysed with 1× Laemmli sample buffer (100 μl per well of 12-wells plate). After scraping, the extracts were forced back and forward through a narrow gauge needle, microcentrifuged, and incubated for 5 min at 95 °C. The samples were then subjected to SDS-PAGE on 10% acrylamide gels followed by immunoblotting.

For the disruption of lipid rafts, cells were pretreated for 30 min at 37 °C with 10 mM methyl-β-cyclodextrin [6]. Subsequently, cells were treated for 5 min at 37 °C with either medium alone, uPA 10 nM, or 10% bovine fetal serum, in the absence or presence of 10 mM methyl-β-cyclodextrin. Then cells were treated as mentioned above.

2.7. Immunoprecipitation experiments

To analyse specific lipid composition, pools of 600 μl from fractions 2+3 (DRM) and 7+8 (DS) obtained from the [1-^{3}H]sphingosine labelled cell lysates were precleared with Dynabeads-protein G for 2 h and then subjected to immunoprecipitation with a monoclonal anti uPAR antibody (R4) that had been precoupled to Dynabeads-protein G, overnight at 4 °C. Parallel experiments were made with non-reactive mouse IgG as negative control. After washing 3 times with lysis buffer, lipids were extracted from the immunoprecipitates with chloroform/methanol 2:1 (v/v) and analyzed as described below. Proteins were eluted from the beads with sample buffer under denaturating conditions, and subjected to SDS-PAGE and immunoblotting for uPAR detection.

To quantitate uPAR in the various fractions, pools of 600 μl from fractions 2+3 (DRM) and 7+8 (DS) obtained from the [^{35}S]-methionine labelled cell lysates were precleared with Sepharose-protein G for 2 h and then subjected to immunoprecipitation with a monoclonal anti uPAR antibody (R4) that had been precoupled to Sepharose-protein G, overnight at 4 °C. Parallel experiments were made with non-reactive mouse IgG as negative control. After washing 3 times with lysis buffer, the amount of radioactivity present in the immunoprecipitate was determined. Then, the samples were subjected to SDS-PAGE and autoradiography.

2.8. Analysis of radioactive lipids

The cell lysate, post-nuclear supernatant and sucrose gradient fractions obtained after [1-^{3}H]sphingosine cell metabolic radiolabeling were analyzed to determine the content of radiolabelled lipids [12]. Samples were dialyzed for 3 days against distilled and decarbonated water. Then, samples were lyophilized, and lipids were extracted twice with 0.5 ml chloroform/methanol 2:1 (v/v) [26]. Aliquots of the lipid extracts were analyzed by HPTLC as described below, followed by radioactivity imaging for quantification. Identity of lipids separated by HPTLC was assessed by co-migration with purified molecular standards.

2.9. Thin layer chromatography

Tritiated lipids were separated by one-dimensional HPTLC carried out with the solvent systems chloroform/methanol/0.2% aqueous $CaCl_2$ 55:45:10 v/v/v, followed by radioactivity imaging for quantification of radioactivity. In some cases, lipids were also separated by two-dimensional HPTLC, using chloroform/methanol/water, 110:40:6 (v/v/v) as the solvent system for the first run, and chloroform/methanol/0.2% aqueous $CaCl_2$, 55:45:10 (v/v/v) for the second run. Cholesterol in the lipid extracts was separated by one-dimensional HPTLC using the solvent system hexane/ethyl acetate, 3:2 (v/v). Cholesterol was quantified after separation on HPTLC by visualization with 15% concentrated sulphuric acid in 1-butanol.

2.10. Other analytical methods

The protein content was determined according to Lowry [44], or with the micro BCA assays (Pierce Chemical Co.), using bovine serum albumin in the presence of sucrose as the reference standard.

The radioactivity associated with whole cells, cell fractions, immunoprecipitation samples, lipids and delipidized pellets was determined by liquid scintillation counting. Digital autoradiography of the HPTLC plates was performed with a Beta-Imager 2000 instrument (Biospace, Paris) using an acquisition time of about 24 h. The radioactivity associated with individual lipids was determined with the specific β-Vision software provided by Biospace.

3. Results

3.1. UPAR is enriched in detergent-resistant membranes obtained from HEK 293-uPAR cells

It has been previously reported that uPAR can be isolated from cell membranes in association with Triton X-100-resistant low-density membranes [6,7]. As a first approach to identify and characterize the plasma membrane domains in which uPAR is located, we used HEK 293-uPAR cells that do not produce uPA, performed sucrose density gradients on the Triton X-100 (TX-100) extract and analyzed uPAR association with DRM, i.e. fractions 2–3 of the gradient, and DS (detergent-soluble material, i.e. fractions 7–8).

We first compared the distribution of total proteins and uPAR in the different fractions of sucrose density gradients. HEK 293 cells, stably transfected with human uPAR (HEK293-uPAR, [6]) were incubated in methionine-free medium for 2 h and subsequently supplemented with 17 μCi/ml L-[^{35}S]methionine for 20 h. After metabolic radiolabeling, cells were lysed in 1% TX-100 and then the lysates were subjected to ultracentrifugation on sucrose gradients and separated into 8 fractions. Fractions were counted for ^{35}S content and analyzed by SDS-

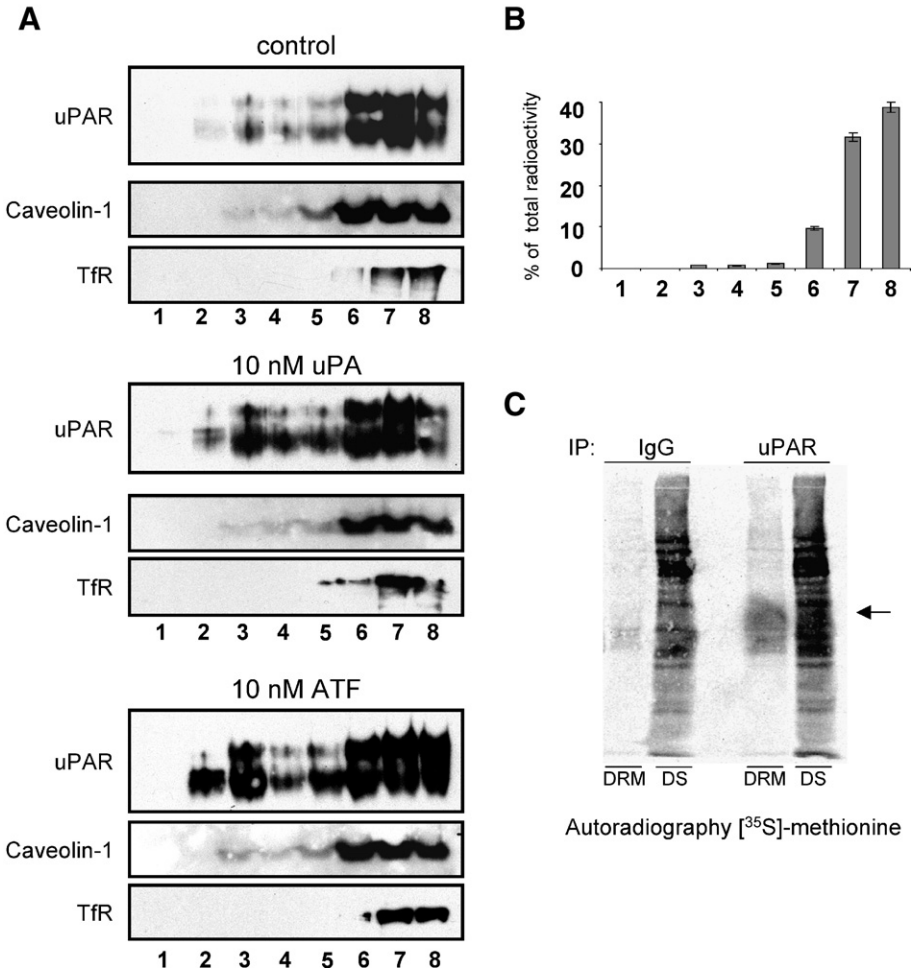

Fig. 1. uPAR associates with DRM. Cells were lysed in the presence of TX-100 at 4 °C. DRM were purified by sucrose gradient centrifugation as described in material and methods. One ml fractions were collected from the top (fraction 1) to bottom (fraction 8). Panel A: proteins were analyzed by SDS-PAGE and Western blotting using specific anti-uPAR, anti-caveolin-1 and anti TfR antibodies, respectively. Upper panel: control cells. Middle panel: cells treated with 10 nM uPA for 5 min at 37 °C. Lower panel: cells treated with 10 nM ATF for 5 min at 37 °C. Data are representative of 3 independent experiments. Panel B: in control cells, metabolic labelling of cell proteins with [^{35}S]methionine was performed before DRM separation. The amount of protein-associated radioactivity was determined by liquid scintillation counting. Data are expressed as percentage of total radioactivity present in the lysate. Panel C: DRM and DS were obtained by sucrose gradient centrifugation from control (untreated) cells and subjected to immunoprecipitation performed at 4 °C using anti-uPAR antibodies. Non-reactive IgG were used as negative control. Samples were separated by SDS-PAGE and then transferred on a PVDF membrane. [^{35}S]methionine-labelled cell proteins immunoprecipitated with anti-uPAR antibodies or non-reactive IgG were detected by autoradiography. The band corresponding to uPAR is indicated with an arrow.

PAGE and immunoblotting. Fig. 1A (Upper Panel) shows that uPAR was present in the DRM (lanes 2 and 3), which contained less than 1% of the total [^{35}S]proteins (Fig. 1B). Caveolin-1, in fact showed a similar distribution. On the other hand, TfR partitioned exclusively in the DS membrane fractions of the gradient, which also contained the majority of uPAR (Fig. 1A, Upper Panel, lanes 6–8). Besides, the DS fractions contained more than 70% of the total cell protein radioactivity (Fig. 1B). Immunoprecipitation of uPAR from the DRM and DS fractions isolated from L-[^{35}S]-methionine labelled-cells (Fig. 1C, arrow) and counting of the precipitated radioactivity showed that uPAR was highly enriched in these fractions (close to hundred fold), while constituting only 0.03% of the total proteins (Table 1). The heterogeneous glycosylation pattern and the presence of both full-length and truncated forms (D2D3 forms) of uPAR, account for the double, enlarged and fuzzy band of Fig. 1C [4,5].

3.2. UPA binding increases uPAR association to detergent-resistant membranes independently of its catalytic activity

It has been widely described that uPA binding to uPAR induces both proteolysis-dependent and independent intracellular signalling events that affect adhesion, migration, and proliferation in a variety of cells [5]. Here, we studied whether uPA plays a role in uPAR localization to lipid rafts. HEK 293-uPAR cells were incubated either with 10 nM uPA or ATF (the Amino Terminal Fragment of uPA that binds to the receptor but lacks the catalytic domain) for 5 min at 37 °C, enough to saturate cell surface uPAR [5] and to induce intracellular signalling (see below). After the incubation period, cells were lysed in 1% TX-100 and treated as described above. Interestingly, after uPA binding there was a three-fold increase in uPAR content in the DRM (i.e. from about 5% to about 15%,

Table 1
Distribution of ^{35}S radioactivity after immunoprecipitation with anti-uPAR or non specific (control) IgG in DRM and DS fractions

Material	Antibodies	Input	IP [a]	Preclear	Supernatant	uPAR enrichment (%) [b]
DRM	IgG anti		7567			
	uPAR non-reactive	128767	(5.15%, sp.)	1639	109700	85.8
DRM	IgG	128767	991	1411	112567	NP
	IgG anti		44898			
DS	uPAR non-reactive	5473752	(0.06%, sp.)	22022	5389167	1
DS	IgG	5473752	12018	25800	5426897	NP

Cell proteins were previously metabolically labelled with [^{35}S]-methionine. Data are expressed in cpm unless specified. The [^{35}S]-methionine uptake by the cells was of 21,920,000 cpm in total , which is considered as 100% of total cell proteins; of this about one quarter was used in this specific experiment. In additional experiments, the same results were obtained.

[a] The percent uPAR after immunoprecipitation is calculated after subtraction of the non specific (pre-clear), and indicated with "sp".

[b] The fold enrichment of uPAR is calculated by dividing the percent of specific uPAR precipitated from DRM divided by the percent precipitated from the DS fraction.

Fig. 1A, middle panel, lanes 2 and 3), while TfR and caveolin-1 maintained the same distribution pattern (Fig. 1A). An increase in uPAR association to DRM is also observed after ATF binding, suggesting that this event is independent of the catalytic activity of uPA (Fig. 1A, lower panel, lanes 2 and 3).

3.3. Disruption of lipid rafts completely prevents uPA/uPAR intracellular signalling

To investigate the relevance of uPAR localization in lipid microdomains we tested the rate of ERK phosphorylation in conditions in which we previously demonstrated that lipid rafts are disrupted, and uPAR is found exclusively in the DS membrane fractions (not shown, but see [6]). First, we analyzed the rate of ERK phosphorylation induced by uPA at different time points. As shown in Fig. 2A, uPA induces ERK phosphorylation within 1 min. This activation is transient, since the phosphorylated ERK returns to basal levels in less than 15 min. Then, we compared the rate of ERK phosphorylation induced by uPA in untreated or 10 mM CD-treated HEK293-uPAR cells. Under the last condition uPAR is found exclusively in the DS membrane fractions (not shown and [6]). Stimulation with serum, another inducer of ERK that does not act through uPAR, was used as control. As shown in Fig. 2B, uPA induced ERK phosphorylation in untreated cells after 5 min of incubation, whereas CD-treatment prevented ERK phosphorylation altogether. Unlike uPA, the treatment of cells with CD had no effect on the serum-induced ERK phosphorylation (Fig. 2B). This result is also in agreement with previously reported data on the same cells in which CD treatment specifically blocked uPAR-dependent, but not integrin-dependent, adhesion on vitronectin [6]. Thus, we conclude that the presence of uPAR in lipid microdomains is relevant for its signalling function. On these premises, we have decided to analyze the lipid composition of the uPAR-containing microdomains and test whether uPA binding would induce any change in the lipid microdomains.

3.4. UPAR associates with sphingolipid and cholesterol-enriched detergent-resistant membranes

To characterize the lipid composition of uPAR membrane microdomain, sphingolipids were metabolically labelled with [1-^{3}H]sphingosine. [1-^{3}H]sphingosine is rapidly taken up by cultured cells and is efficiently converted into complex sphingolipids. Moreover, it is in part catabolized to tritiated ethanolamine, that is recycled for the biosynthesis of phosphatidylethanolamine (PE), a glycerophospholipid that can be conveniently used as a marker of non-DRM fractions [12,17]. After metabolic radiolabeling, cells were first incubated with 10 nM uPA or ATF for 5 min at 37 °C and then lysed in 1% TX-100. The lysates were subjected to ultracentrifugation on sucrose gradients and separated into 8 fractions. The radioactive lipids were extracted, separated by HPTLC and analyzed by radioimaging. The radioactive lipid patterns of the gradient fractions and the quantitative distribution of radioactive sphingolipids and PE are not shown but are available in Suppl. Figure 1. No statistically significant differences were observed between cells incubated with medium alone, uPA or ATF. The DRM fractions contained about 25% of cellular sphingolipids (25.3 and 24.8% for control and uPA-treated, 20.6% for ATF-treated cells), in particular sphingomyelin (the major SL present in these cells), ceramide, LacCer, GM2 and GM3, and other minor SL. PE, as

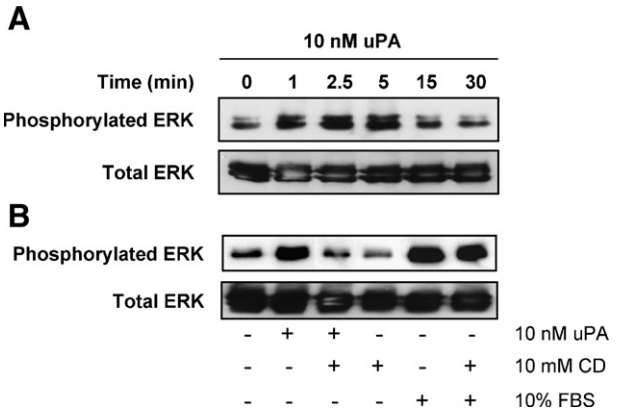

Fig. 2. Disruption of lipid rafts abolishes uPA-induced ERK phosphorylation. (A) HEK 293-uPAR cells were serum-starved for 16 h and then treated with 10 nM uPA at 37 °C for the indicated times. Phosphorylated and total ERK were detected by immunoblot analysis. The Western blots are representative of three independent experiments. (B) HEK 293-uPAR cells were serum-starved for 16 h and then pre-treated with 10 mM CD at 37 °C. After 30 min, cells were incubated for another 5 min at 37 °C with 10 nM uPA, 10% FBS, or medium alone, in the absence or presence of 10 mM CD, as indicated. Phosphorylated and total ERK were detected as described in Materials and methods.

expected, was located mainly in the DS membrane fractions of the gradient (Suppl. Figure 1). The other major lipid component of membrane lipid domains is cholesterol. Thus, we also checked the distribution of cholesterol in the gradient. Again, about 25% of total cellular cholesterol was found in DRM independently of the presence of uPAR ligands (Suppl. Figure 1). These results demonstrate that binding of uPA or ATF does not lead to an overall modification of the lipid composition of the DRM.

3.5. UPA binding modifies the lipid composition of uPAR membrane microdomain independently of its catalytic activity

Since uPAR associates to lipid rafts, and this association is increased after uPA binding, we determined the sphingolipid content of the uPAR membrane microdomains at steady state and after uPA binding. For this purpose, pooled DRM fractions (fractions 2 and 3) from the sucrose density gradients shown in Fig. 1 and Suppl. Figure 1 were subjected to immunoprecipitation with the anti-uPAR monoclonal antibody R4, under conditions designed to preserve the integrity of the domains (see Methods section) [18]. We also used non-reactive IgG as a negative control. By Western blot assays we determined that the immunoprecipitates performed with R4 contained the uPAR associated to DRM (Fig. 3). In control, uPA, and ATF-treated cells, uPAR was present in both the full length and the cleaved (D2D3) forms. However, no uPAR was found in the precipitate with non-reactive IgG. The presence of D2D3 form is in keeping with the higher sensitivity of DRM-uPAR (as opposed to DS-uPAR) to cleavage by uPA or other endogenous protease [6].

The specific (R4 antibody) immunoprecipitate contained about 10% (from 8.8 to 11%) of the total tritium labelled sphingolipids associated to DRM, in the three conditions tested (control, uPA- or ATF-treated, Table 2). Less than 0.5% of the total tritium labelling was associated with the non-reactive IgG and with the protein G-coupled magnetic beads used to preclear the samples (Table 2). No uPAR was detected with the protein G-coupled magnetic beads alone (not shown). The recovery was higher than 85% in all the samples.

It is worth mentioning that when the DS fractions obtained from the sucrose density gradients of Fig. 1 and Suppl. Figure 1 were subjected to immunoprecipitation with the antibody R4, uPAR was effectively precipitated, but the immunoprecipitates

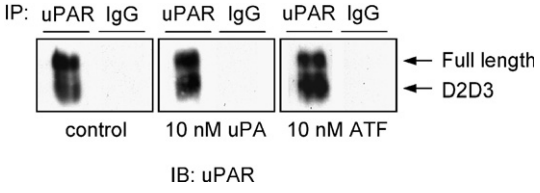

Fig. 3. Immunoprecipitation of uPAR from the DRM. DRM was prepared by sucrose gradient centrifugation from control cells (left), cells treated with 10 nM uPA (middle) or with 10 nM ATF (right) for 5 min at 37 °C, and subjected to immunoprecipitation performed at 4 °C using anti-uPAR antibodies (lane 1). Non-reactive IgG were used as negative control. Samples were separated by SDS-PAGE and then transferred on a PVDF membrane. uPAR was visualized by Western blotting with specific antibodies.

Table 2
Distribution of [^{3}H] radioactivity after immunoprecipitation with anti-uPAR or non-reactive (control) IgG in sphingolipid-enriched membrane fractions of control, or uPA/ATF treated cells

Material	Addition	Input	IP [a]	Preclear	% [^{3}H] sp precipitated [b]
Anti uPAR	none	17812	1621.5	0	8.8
Non-reactive IgG	none	17812	54.4	11.9	
Anti uPAR	uPA	14875.5	1441	46.8	9.2
Non-reactive IgG	uPA	14875.5	72.5	0	
Anti uPAR	ATF	17873.5	2026.5	33.1	11.2
Non-reactive IgG	ATF	17873.5	60.4	0.9	

Cell lipids were previously metabolically labelled with [^{3}H]-sphingosine. Data are expressed in dpm unless specified.

[a] The immunoprecipitate was performed with the R4 antibody or with a non-reactive isotypic control.

[b] The percent of input radioactivity is calculated after subtraction of the amount precipitated from the non reactive IgG.

contained less than 2% of the radioactive lipids present in the DS fractions, mainly represented by PE (data not shown).

Tritiated lipids extracted from the uPAR immunoprecipitates were analyzed by two-dimensional HPTLC and compared to those from the DRM (Fig. 4). The DRM from cells incubated with medium alone, uPA or ATF contained sphingomyelin, gangliosides GM2 and GM3, neutral glycosphingolipids GlcCer and LacCer, and ceramide (Fig. 4A, left panel). The two-dimensional lipid patterns of the DRM in control, uPA- and ATF-treated cells were very similar. Moreover, the lipid composition of the uPAR immunoprecipitate in control cells did not significantly differ from that of the total DRM (Fig. 4A, upper panel). However, in the uPAR immunoprecipitates from both uPA- and ATF-treated cells (Fig. 4A, middle and lower panels), we found a much lower amount of neutral glycosphingolipids, which remained in the supernatant. After quantitative determination of the radioactivity associated with each spot, we found a 60% reduction in neutral glycosphingolipids in the uPAR immunoprecipitates from both uPA- and ATF-treated cells (Fig. 4B). In these same immunoprecipitates, we found a 1.5 fold increase in GM2 and GM3 (Fig. 4B). These results suggest that uPA binding modifies the lipid composition of uPAR membrane microdomains, and that this modification is independent of the catalytic activity of uPA.

4. Discussion

UPAR is a GPI anchored protein that can promote signal transduction events inside the cell independently of the catalytic activity of uPA [5]. The intracellular signalling process may be triggered by the association of uPAR to other proteins such as vitronectin [20], integrins [21], FPRL1 [22], caveolin-1 [7,19], EGF-R (Epidermal Growth Factor Receptor) [23] and LRP-1 (low-density lipoprotein–receptor-related protein) [24]. Since uPAR is located in different compartments at the cell surface, the microenvironment, i.e., the surrounding lipids and proteins, should be important to control uPAR function. UPAR, as many other GPI-anchored proteins [15,25], is partially localized in lipid rafts or lipid membrane microdomains, zones of the membrane particularly enriched in cholesterol and sphingolipids, being therefore partially insoluble in TX-100, and sensitive to cholesterol

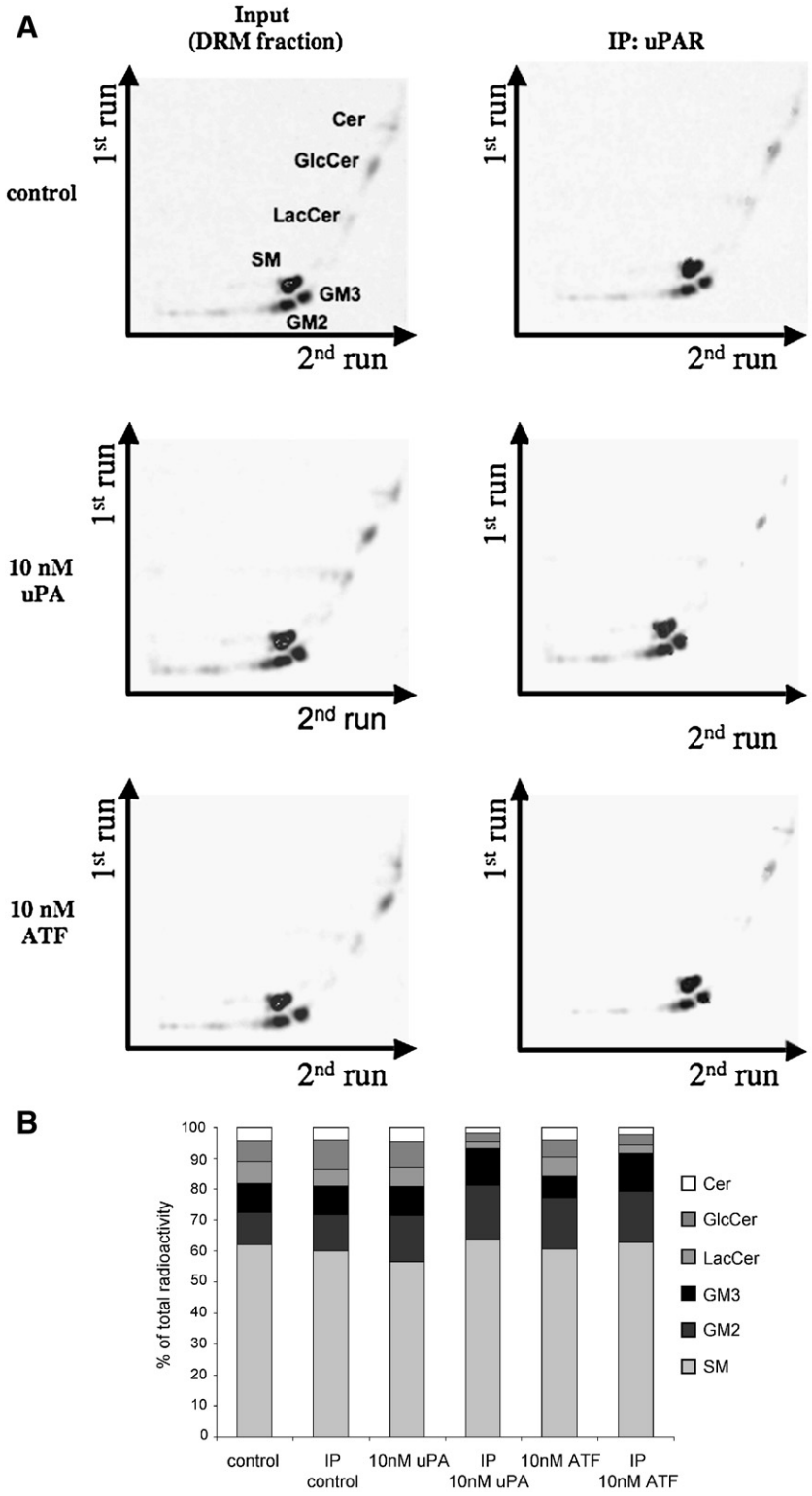

Fig. 4. Sphingolipid composition of uPAR membrane microdomain. (A) Two-dimensional HPTLC patterns of radioactive lipids present in uPAR immunoprecipitates from DRM. Cell lipids were metabolically labelled with [1-^{3}H]sphingosine, (2 h pulse followed by 48 h chase). DRM were prepared by sucrose gradient centrifugation from control cells, cells treated with 10 nM uPA or with 10 nM ATF for 5 min at 37 °C, and subjected to immunoprecipitation performed at 4 °C using anti-uPAR antibodies. Radioactive lipids from DRM and from anti uPAR immunoprecipitates were extracted and separated by 2D-HPTLC using the solvent systems: 1st run, chloroform/methanol/water, 110:40:6 by vol; 2nd run, chloroform/methanol/0.2% aqueous $CaCl_2$, 50:42:11 by vol. Radioactive lipids were detected by digital autoradiography; 500–2000 dpm/plate; time of acquisition: 65 h. Upper panel: control cells. Middle panel: cells treated with 10 nM uPA for 5 min at 37 °C. Lower Panel: cells treated with 10 nM ATF for 5 min at 37 °C. Right panel: total DRM (input). Left panel: anti uPAR immunoprecipitates. Patterns are representative of those obtained in three different experiments. (B) Quantitative analysis of the lipid composition in the anti-uPAR immunoprecipitated microdomain. The amount of radioactivity associated with each spot shown in A was determined with the specific β-Vision software provided by Biospace. The data are expressed as percent of total ^{3}H radioactivity present in the plates for the three conditions tested (control, 10 nM uPA or 10 nM ATF).

depletion [6,7]. The GPI anchor is responsible for uPAR insolubility in TX-100, since a chimeric uPAR mutant, bearing the EGFR transmembrane domain in place of its GPI anchor consensus sequence, does not partition to lipid membrane domains [6].

Lipid and protein organization at the cell surface is considered to play a crucial role in modulating functional processes, such as those associated with uPAR, and favouring their compartmentalization. This idea is supported by our experiments with CD. Indeed, after CD treatment, lipid rafts are disrupted and the uPA-dependent induction of ERK phosphorylation is completely inhibited. This is a specific effect for the uPA/uPAR system, since other signals that do not go via lipid rafts are insensitive to CD (Fig. 2). The specific adhesion of HEK239-uPAR cells onto vitronectin was also reported to be totally dependent on lipid microdomains integrity [6]. These data confirm the expected importance of lipid rafts in uPAR intracellular signalling. However, no data were available concerning the lipid composition of uPAR environment in lipid rafts. Our results show that in HEK293-uPAR cells, uPAR is partially associated to DRM, and that the association to DRM increases after ligand binding. In the absence of ligand, uPAR is located in a lipid environment very similar to that of total DRM, enriched in sphingomyelin and glycosphingolipids. However, after treatment of cells with uPA or ATF the specific lipid environment is impoverished of neutral glycosphingolipids with relative increases of sphingomyelin and gangliosides (Fig. 4).

Although many receptors are localized in lipid rafts, the effect of the ligand in this association is highly variable. For example, the insulin receptor is recruited to lipid rafts after insulin binding [27], while the β_2-adrenergic receptor moves out of lipid rafts after agonist binding [28]. However, the functional implications of such changes in receptor compartmentalization are unclear. In our system, even if uPAR is already localized in lipid microdomains, more receptor is recruited into lipid rafts in the presence of its specific ligand uPA. A similar increase of uPAR association to lipid rafts is observed after ATF binding. Since ATF binds to the receptor but lacks the catalytic activity, it is the binding of uPA to uPAR but not the associated cell surface proteolysis that is required for receptor recruitment into lipid rafts. Moreover, the microenvironment of the lipid rafts in which uPAR is located changes after ligand binding. It has been proposed that by modulating the entrance of some proteins, lipid rafts can control intracellular signalling [16]. In this sense, increasing the amount of uPAR in lipid rafts after uPA binding might trigger or enhance the uPA/uPAR-related signalling activation that control cell adhesion, migration, proliferation and differentiation. Here we showed that the presence of uPAR in lipid rafts is essential for uPA/uPAR-induced ERK phosphorylation. Previously, it has been shown that the localization of uPAR and uPA in caveolae enhances pericellular plasminogen activation [7]. Other data show that dimeric uPAR partitions preferentially to lipid rafts, where it binds to vitronectin in a way that can be blocked by cholesterol depletion [6]. While uPA binds to uPAR independently of its membrane localization and dimerization status, uPA-induced uPAR cleavage is strongly accelerated in lipid rafts [6].

Our results support the idea that a protein can belong to distinct lipid membrane domains, since the SL microenvironment in which uPAR is located changes after uPA binding. In fact it has been reported that after certain stimuli, uPAR can segregate at the leading edge of a migrating T-cell in GM3-enriched lipid rafts rather than GM1-enriched lipid rafts localized at the uropod [29]. In addition to the specific lipid composition changes induced by the ligands, we also find by confocal fluorescence and co-immunoprecipitation experiments (not shown) that uPAR does not co-localize with caveolin-1 in the plasma membrane of HEK293-uPAR cells. In fact, co-localization between uPAR and caveolin is found only in the Golgi (Cortese et al., in preparation). This finding also eliminates any doubt that the DRM fractions that we have analyzed may contain not only plasma membrane but also Golgi and other organelles membranes.

After receptor activation by ligand binding, the uPAR-immunoprecipitate was enriched in gangliosides and sphingomyelin. Gangliosides are found in the outer layer of the plasma membrane and are involved in a number of biological processes such as cell adhesion, signal transduction, tumorigenesis, differentiation and metastasis [30,31]. As one of the gangliosides enriched in the uPAR-immunoprecipitate was GM3, it could be speculated that the GM3 enrichment after uPA binding might be relevant in the role that uPAR plays in cell processes as GM3 is involved in cell motility/invasiveness [32] and EGFR dimerization and autophosphorylation [33–36]. This might be relevant since, as mentioned before, EGFR and uPAR can modulate each others activity [23,37]. However, additional studies are required to understand the functional role of GM3 enrichment in lipid raft under cellular events regulated by the uPA/uPAR system. This result is intriguing since the generation of the second messenger ceramide from SM has been suggested to occur preferentially in lipid rafts upon certain stimuli. On a speculative basis, this local change in the SL content may modify raft functioning, triggering signalling events and allowing receptor oligomerization [38,39]. In addition, we found that neutral glycosphingolipids were diminished in the uPAR-enriched lipid rafts. According to these results, it could be hypothesized that neutral glycosphingolipids might restrict the presence of uPAR in lipid rafts from resting cells. Again, additional studies are required in order to test this hypothesis.

Altogether, these results suggest that uPAR is located in specific subdomains within lipid rafts, with characteristic lipid composition. The localization of the receptor as well as the composition of the subdomains is regulated by ligand binding. Hypothetically, this microenvironment might modify uPAR specific responses. Neutral glycosphingolipids might restrict the presence of uPAR in lipid rafts, while SM and ceramide could induce intracellular signalling cascades, and GM2 and GM3 might facilitate the association with other receptors and signalling molecules. Our findings shed light not only in the relevance of the localization of uPAR in lipid rafts, but also show the important role that lipid rafts themselves play in the selectivity and compartmentalization of cell processes.

Acknowledgements

This work was supported by FIRB (2001) of the Italian Ministry of University and Research, AIRC (Italian Association for Cancer Research), EU IP Cancer-Degradome and NoE MAIN to FB, and by COFIN-PRIN (2002, 2003 and 2004), FIRST (2002, 2003 and 2004) and FIRB (2001) to A.P and S.S., Italy. M. Sahores was supported by a grant of the Italian-Argentinean Cooperation Program SECyT-MAE (IT/PA03-SV/051) and G.C. by CONICET (Concejo Nacional de Investigaciones Científicas y Técnicas, Argentina) and FONCyT: BID 1728/OC-AR PICT No. 05-13945 (Agencia Nacional de Ciencia de la República Argentina).

Appendix A. Supplementary data

Supplementary data associated with this article can be found, in the online version, at doi:10.1016/j.bbamem.2007.09.030.

References

[1] L. Svennerholm, Ganglioside designation, Adv. Exp. Med. Biol. 125 (1980) 11.
[2] IUPAC-IUBMB & Nomenclature, J.C.o.B., Pure Appl. Chem. 69 (1997) 2475–2487.
[3] IUPAC-IUBMB & Nomenclature, J.C.o.B., Carbohydr. Res. 312 (1998) 167–175.
[4] M. Ploug, E. Ronne, N. Behrendt, A.L. Jensen, F. Blasi, K. Dano, Cellular receptor for urokinase plasminogen activator. Carboxyl-terminal processing and membrane anchoring by glycosyl-phosphatidylinositol, J. Biol. Chem. 266 (1991) 1926–1933.
[5] F. Blasi, P. Carmeliet, uPAR: a versatile signalling orchestrator, Nat. Rev., Mol. Cell Biol. 3 (2002) 932–943.
[6] O. Cunningham, A. Andolfo, M.L. Santovito, L. Iuzzolino, F. Blasi, N. Sidenius, Dimerization controls the lipid raft partitioning of uPAR/CD87 and regulates its biological functions, EMBO J. 22 (2003) 5994–6003.
[7] A. Stahl, B.M. Mueller, The urokinase-type plasminogen activator receptor, a GPI-linked protein, is localized in caveolae, J. Cell Biol. 129 (1995) 335–344.
[8] D.A. Brown, J.K. Rose, Sorting of GPI-anchored proteins to glycolipid-enriched membrane subdomains during transport to the apical cell surface, Cell 68 (1992) 533–544.
[9] G. van Meer, K. Simons, Lipid polarity and sorting in epithelial cells, J. Cell. Biochem. 36 (1988) 51–58.
[10] S. Hakomori, K. Handa, K. Iwabuchi, S. Yamamura, A. Prinetti, New insights in glycosphingolipid function: "glycosignaling domain," a cell surface assembly of glycosphingolipids with signal transducer molecules, involved in cell adhesion coupled with signaling, Glycobiology 8 (1998) xi–xix.
[11] A. Prinetti, K. Iwabuchi, S. Hakomori, Glycosphingolipid-enriched signaling domain in mouse neuroblastoma Neuro2a cells. Mechanism of ganglioside-dependent neuritogenesis, J. Biol. Chem. 274 (1999) 20916–20924.
[12] A. Prinetti, V. Chigorno, G. Tettamanti, S. Sonnino, Sphingolipid-enriched membrane domains from rat cerebellar granule cells differentiated in culture. A compositional study, J. Biol. Chem. 275 (2000) 11658–11665.
[13] M.A. Alonso, J. Millan, The role of lipid rafts in signalling and membrane trafficking in T lymphocytes, J. Cell Sci. 114 (2001) 3957–3965.
[14] L.D. Zajchowski, S.M. Robbins, Lipid rafts and little caves. Compartmentalized signalling in membrane microdomains, Eur. J. Biochem. 269 (2002) 737–752.
[15] K. Simons, D. Toomre, Lipid rafts and signal transduction, Nat. Rev., Mol. Cell Biol. 1 (2000) 31–39.
[16] H.A. Lucero, P.W. Robbins, Lipid rafts–protein association and the regulation of protein activity, Arch. Biochem. Biophys. 426 (2004) 208–224.
[17] A. Prinetti, V. Chigorno, S. Prioni, N. Loberto, N. Marano, G. Tettamanti, S. Sonnino, Changes in the lipid turnover, composition, and organization, as sphingolipid-enriched membrane domains, in rat cerebellar granule cells developing in vitro, J. Biol. Chem. 276 (2001) 21136–21145.
[18] A. Prinetti, S. Prioni, V. Chigorno, D. Karagogeos, G. Tettamanti, S. Sonnino, Immunoseparation of sphingolipid-enriched membrane domains enriched in Src family protein tyrosine kinases and in the neuronal adhesion molecule TAG-1 by anti-GD3 ganglioside monoclonal antibody, J. Neurochem. 78 (2001) 1162–1167.
[19] Y. Wei, X. Yang, Q. Liu, J.A. Wilkins, H.A. Chapman, A role for caveolin and the urokinase receptor in integrin-mediated adhesion and signaling, J. Cell Biol. 144 (1999) 1285–1294.
[20] Y. Wei, D.A. Waltz, N. Rao, R.J. Drummond, S. Rosenberg, H.A. Chapman, Identification of the urokinase receptor as an adhesion receptor for vitronectin, J. Biol. Chem. 269 (1994) 32380–32388.
[21] Y. Wei, M. Lukashev, D.I. Simon, S.C. Bodary, S. Rosenberg, M.V. Doyle, H.A. Chapman, Regulation of integrin function by the urokinase receptor, Science 273 (1996) 1551–1555.
[22] M. Resnati, I. Pallavicini, J.M. Wang, J. Oppenheim, C.N. Serhan, M. Romano, F. Blasi, The fibrinolytic receptor for urokinase activates the G protein-coupled chemotactic receptor FPRL1/LXA4R, Proc. Natl. Acad. Sci. U. S. A. 99 (2002) 1359–1364.
[23] D. Liu, J. Aguirre Ghiso, Y. Estrada, L. Ossowski, EGFR is a transducer of the urokinase receptor initiated signal that is required for in vivo growth of a human carcinoma, Cancer Cell 1 (2002) 445–457.
[24] A. Nykjaer, C.M. Petersen, B. Moller, P.H. Jensen, S.K. Moestrup, T.L. Holtet, M. Etzerodt, H.C. Thogersen, M. Munch, P.A. Andreasen, et al., Purified alpha 2-macroglobulin receptor/LDL receptor-related protein binds urokinase.plasminogen activator inhibitor type-1 complex. Evidence that the alpha 2-macroglobulin receptor mediates cellular degradation of urokinase receptor-bound complexes, J. Biol. Chem. 267 (1992) 14543–14546.
[25] S. Sabharanjak, S. Mayor, Folate receptor endocytosis and trafficking, Adv. Drug Deliv. Rev. 56 (2004) 1099–1109.
[26] L. Riboni, R. Bassi, S. Sonnino, G. Tettamanti, Formation of free sphingosine and ceramide from exogenous ganglioside GM1 by cerebellar granule cells in culture, FEBS Lett. 300 (1992) 188–192.
[27] S. Vainio, S. Heino, J.E. Mansson, P. Fredman, E. Kuismanen, O. Vaarala, E. Ikonen, Dynamic association of human insulin receptor with lipid rafts in cells lacking caveolae, EMBO Rep. 3 (2002) 95–100.
[28] V.O. Rybin, X. Xu, M.P. Lisanti, S.F. Steinberg, Differential targeting of beta -adrenergic receptor subtypes and adenylyl cyclase to cardiomyocyte caveolae. A mechanism to functionally regulate the cAMP signaling pathway, J. Biol. Chem. 275 (2000) 41447–41457.
[29] C. Gomez-Mouton, J.L. Abad, E. Mira, R.A. Lacalle, E. Gallardo, S. Jimenez-Baranda, I. Illa, A. Bernad, S. Manes, A.C. Martinez, Segregation of leading-edge and uropod components into specific lipid rafts during T cell polarization, Proc. Natl. Acad. Sci. U. S. A. 98 (2001) 9642–9647.
[30] S. Hakomori, Glycosylation defining cancer malignancy: new wine in an old bottle, Proc. Natl. Acad. Sci. U. S. A. 99 (2002) 10231–10233.
[31] M.G. Manfredi, S. Lim, K.P. Claffey, T.N. Seyfried, Gangliosides influence angiogenesis in an experimental mouse brain tumor, Cancer Res. 59 (1999) 5392–5397.
[32] M. Ono, K. Handa, D.A. Withers, S. Hakomori, Motility inhibition and apoptosis are induced by metastasis-suppressing gene product CD82 and its analogue CD9, with concurrent glycosylation, Cancer Res. 59 (1999) 2335–2339.
[33] A.R. Zurita, H.J. Maccioni, J.L. Daniotti, Modulation of epidermal growth factor receptor phosphorylation by endogenously expressed gangliosides, Biochem. J. 355 (2001) 465–472.
[34] P.M. Crespo, A.R. Zurita, J.L. Daniotti, Effect of gangliosides on the distribution of a glycosylphosphatidylinositol-anchored protein in plasma membrane from Chinese hamster ovary-K1 cells, J. Biol. Chem. 277 (2002) 44731–44739.
[35] E.A. Miljan, E.G. Bremer, Regulation of growth factor receptors by gangliosides, Sci. STKE 2002 (2002) RE15.
[36] E.A. Miljan, E.J. Meuillet, B. Mania-Farnell, D. George, H. Yamamoto, H.G. Simon, E.G. Bremer, Interaction of the extracellular domain of the epidermal growth factor receptor with gangliosides, J. Biol. Chem. 277 (2002) 10108–10113.

[37] J. Guerrero, J.F. Santibanez, A. Gonzalez, J. Martinez, EGF receptor transactivation by urokinase receptor stimulus through a mechanism involving Src and matrix metalloproteinases, Exp. Cell Res. 292 (2004) 201–208.
[38] H. Grassme, V. Jendrossek, J. Bock, A. Riehle, E. Gulbins, Ceramide-rich membrane rafts mediate CD40 clustering, J. Immunol. 168 (2002) 298–307.
[39] E. Gulbins, R. Kolesnick, Raft ceramide in molecular medicine, Oncogene 22 (2003) 7070–7077.
[40] H.E. Carter, J.A. Rothfus, R. Gigg, Biochemistry of the sphingolipids: XII. conversion of cerebrosides to ceramides and sphingosine; structure of Gaucher cerebroside, J. Lipid Res. 2 (1961) 228–234.
[41] T. Toyokuni, M. Nisar, B. Dean, S. Hakomori, A facile and regiospecific titration of sphingosine: synthesis of (2S,3R,4E)-2-amino-4-octadene-1,3-diol-1-3H, J. Labelled Compd Radiopharm. 29 (1991) 567–574.
[42] G. Tettamanti, F. Bonali, S. Marchesini, V. Zambotti, A new procedure for the extraction, purification and fractionation of brain gangliosides, Biochim. Biophys. Acta 296 (1973) 160–170.
[43] V. Chigorno, C. Riva, M. Valsecchi, M. Nicolini, P. Brocca, S. Sonnino, Metabolic processing of gangliosides by human fibroblasts in culture-formation and recycling of separate pools of sphingosine, Eur. J. Biochem. 250 (1997) 661–669.
[44] O.H. Lowry, N.J. Rosebrough, A.L. Farr, R.J. Randall, Protein measurement with the Folin phenol reagent, J. Biol. Chem. 193 (1951) 265–275.